Simple Electrochemical Procedure for Measuring the Rates of Electron Transfer across Liquid/Liquid Interfaces Formed by Coating Graphite Electrodes with Thin Layers of Nitrobenzene

Chunnian Shi and Fred C. Anson*

Arthur Amos Noyes Laboratories, Division of Chemistry and Chemical Engineering, California Institute of Technology, Pasadena, California 91125

Received: June 12, 1998; In Final Form: September 28, 1998

A simple, new method is described that allows the rates of electron transfer across liquid/liquid interfaces to be measured with unprecedented ease. The method takes advantage of thin layers of organic liquids that adhere to the surface of pyrolytic graphite electrodes. The method was applied to the nitrobenzene/water interface. Redox reactants dissolved in the nitrobenzene included decamethylferrocene and zinc tetraphenylporphyrin. Reactants in the adjoining aqueous phase were multiply charged anions, including $Fe(CN)_6^{3-/4-}$, $Ru(CN)_6^{4-}$, $Mo(CN)_8^{4-}$, and $IrCl_6^{2-}$. Rate constants for cross-phase electron transfer were evaluated and compared with those obtained in recent studies that employed the scanning electrochemical microscope that was invented and developed by A. J. Bard and co-workers.

The examination of electron transfer across interfaces separating two immiscible liquids has received increasing attention in the past decade.[1] One of the newest experimental methods that has been used to measure the rates of such electron-transfer processes is scanning electrochemical microscopy (SECM), a technique invented and extensively applied by Bard and coworkers.[2] In recent applications of SECM to evaluate electron transfer rates at liquid/liquid interfaces[3] the advantages of the technique compared with previously employed methods were pointed out.[3a] Although SECM has many attractive features, it requires a carefully constructed apparatus to control and measure separations in the range of a few micrometers between a microelectrode tip and the interface of interest. In addition, it is usually necessary to resort to curve fitting procedures to obtain kinetic parameters from the experimental data.[3] We have found that a very simple procedure for preparing thin layers of organic liquids on the surface of graphite electrodes, which was used recently to study reactants adsorbed on graphite electrodes,[4] can also be applied to the measurement of rates of electron ransfer at liquid/liquid interfaces. In this report we describe the application of the method to the interface between water and nitrobenzene phases. The simplicity of the method should prove advantageous in cases where the instrumentation required for SECM is not available. The method offers a supplement to the more complex experimental methods employed in earlier studies of electron transfer at liquid/liquid interfaces.[1,5]

The new method is based on the introduction of a thin layer of one phase (nitrobenzene in this report) between the surface of an electrode and a second phase in which the first phase is immiscible (an aqueous electrolyte in this report). The resulting configuration is depicted schematically in Figure 1. Dry, polished, pyrolytic graphite electrodes exhibit sufficient hydrophobic character to cause small volumes of organic liquids such as nitrobenzene (NB) to spread evenly across their surface to produce a thin, adherent layer of the organic phase.[4] Immersion

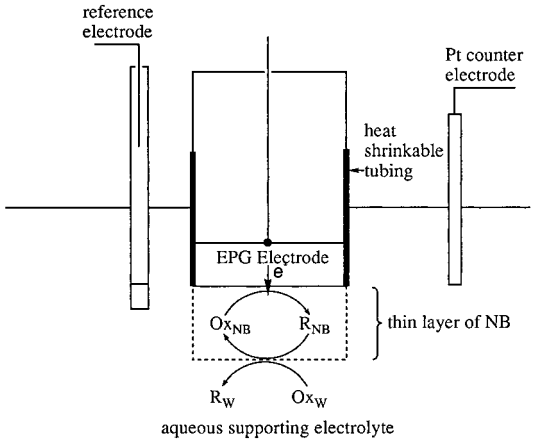

Figure 1. Schematic diagram of the electrochemical cell and the EPG electrode coated with a thin layer of nitrobenzene (NB) employed in this study. The diagram is not to scale. The diameter of the EPG electrode was 0.64 cm, and the thickness of the NB layer was typically 20−30 μm.

of such electrodes in aqueous electrolyte solutions leads to a configuration like the one depicted in Figure 1. With NB as the organic phase, thin layers with thicknesses of 25−30 μm were easily and reproducibly formed. These thin layers proved to be quite stable and were shown to insulate the electrode surface from species in the aqueous phase that do not partition into the organic phase.[4]

If a suitable electroactive reactant is dissolved in the organic liquid used to form the thin layer, it becomes possible to measure steady-state currents at the electrode with magnitudes that can be limited by the rate of electron transfer across the nitrobenzene/water interface. A particularly useful advantage of measuring steady-state currents with the electrode configuration shown in Figure 1 is that no ion transport across the interface accompanies the cross-phase electron transfer. At steady state, electroneutrality in both phases is maintained without ion transport because electrons injected or removed at the electrode/

* Corresponding author. Telephone: 626 395 6000. FAX: 626 405 0454. E-mail: fanson@cco.caltech.edu.

10.1021/jp982605b CCC: $15.00 © 1998 American Chemical Society
Published on Web 11/10/1998

NB interface are removed or injected at exactly the same rate at the NB/H_2O interface and at the H_2O/auxiliary electrode interface. Thus, extraction of electron-transfer rates at the NB/H_2O interface from the measured steady-state currents is unusually straightforward. There is no need for additional experimental manipulations or iterative curve fitting to obtain rate constants. Some examples of the application of this simple procedure are provided in what follows.

Experimental Section

Materials. Cobalt and zinc tetraphenylporphyrins from Porphyrin Products, Inc. (Logan, UT) were purified by column chromatography on neutral alumina. Other chemicals and solvents were of high purity and were used as received. The cylindrical pyrolytic graphite electrodes with 0.32 cm^2 of the edges of the graphitic planes exposed (Union Carbide) were mounted and polished as previously described.[4]

Apparatus and Procedures. Conventional electrochemical cells and instrumentation were employed. Thin layers of NB solutions containing reactants of interest were applied to graphite electrodes held in an upside-down position by transferring 0.8−1.5 μL aliquots of the solutions to the electrode surface with a microsyringe. The organic liquid spread spontaneously across the surface of the graphite. The electrode was then turned over and immediately immersed in the aqueous supporting electrolyte. The stability of the resulting, thin, adherent film of NB was demonstrated previously.[4] Supporting electrolyte in the NB film can be acquired by partitioning of electrolyte from the aqueous phase. From conductance measurements we estimated that 1−3 mM $NaClO_4$ dissolved in NB layers that were equilibrated with aqueous solutions of $NaClO_4$. Even when the concentration of electrolyte in the NB phase was small, the uncompensated resistance introduced by the thin layers of NB was small enough to prevent significant distortions in the shapes of cyclic voltammetric responses from reactants dissolved in the NB.[4] In most cases, a suitable salt, e.g., tetra-*N*-hexylammonium perchlorate (THAP), was dissolved in the nitrobenzene before the thin layer was formed to produce a more conducting organic phase which contained a known concentration of supporting electrolyte.

Results

To demonstrate the simplicity and effectiveness of the use of thin layers of immiscible solvents on graphite electrode surfaces to evaluate electron-transfer rates at the interface between the thin layer and aqueous supporting electrolytes, we examined several such reactions.

Electron Transfer from Decamethylferrocene to $Fe(CN)_6^{3-}$ across the NB/H_2O Interface. Shown in Figure 2A is a cyclic voltammogram recorded at a bare edge plane pyrolytic graphite (EPG) electrode in a 0.5 mM aqueous solution of $Fe(CN)_6^{3-}$ with 0.1 M $NaClO_4$ + 0.1 M NaCl as the supporting electrolyte. When a thin layer of NB was placed on the electrode surface (using the procedure described in the Experimental Section), the voltammetric response from the $Fe(CN)_6^{3-/4-}$ couple disappeared because the $Fe(CN)_6^{3-}$ anions could no longer reach the electrode surface (Figure 2B). In Figure 2C is shown the response obtained when decamethylferrocene (DMFc) was dissolved in the NB before the thin layer was formed on the electrode. The aqueous solution contained only supporting electrolyte. The reversible couple near −0.2 V corresponds to the $DMFc^+$/DMFc couple.[6] This response was quite stable: Repetitive scanning of the potential between +0.3 and −0.4 V produced no significant decrease in the peak currents. The loss

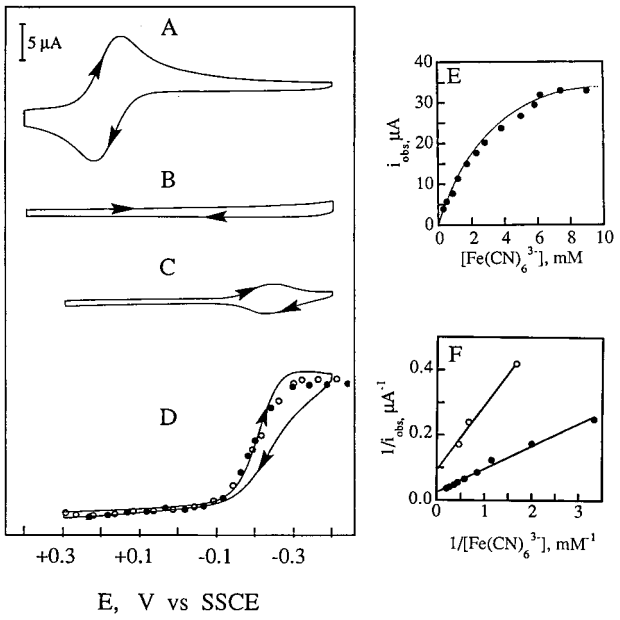

Figure 2. Voltammetric observation of electron-transfer from DMFc in a thin layer of NB to $Fe(CN)_6^{3-}$ in water. (A) Cyclic voltammogram for 0.47 mM $Fe(CN)_6^{3-}$ at an uncoated EPG electrode: supporting electrolyte, 0.1 M $NaClO_4$ + 0.1 M NaCl; scan rate, 5 mV s^{-1} throughout. (B) Repeat of A after the electrode surface was covered with 1 μL of NB. (C) Cyclic voltammogram with the electrode covered with 1 μL of NB containing 0.55 mM $DMFc^+$ (generated by oxidation of DMFc at the initial potential). The aqueous solution contained only supporting electrolyte (0.1 M $NaClO_4$ + 0.1 M NaCl). (D) Solid line: Repeat of C with 1.7 mM $Fe(CN)_6^{3-}$ present in the aqueous phase. The plotted points are the steady-state currents recorded at a scan rate of 0 mV s^{-1} as the potential was stepped to more negative (○) and to more positive (●) values. (E) Cathodic plateau currents such as that in D as a function of the concentration of $Fe(CN)_6^{3-}$ in the aqueous phase. The NB phase contained 0.55 mM $DMFc^+$. (F) Reciprocal plateau currents vs $[Fe(CN)_6^{3-}]^{-1}$ with $[DMFc^+]_{NB}$ = 0.55 (●) or 0.20 (○) mM.

of $DMFc^+$ from the NB layer by partitioning into the aqueous phase became more significant in the absence of ClO_4^- anions, which appear to diminish the solubility of $DMFc^+$ in the aqueous phase. When $Fe(CN)_6^{3-}$ was added to the aqueous phase, the voltammetric response changed, as shown in Figure 2D. The enhanced cathodic current at the potential where the $DMFc^+$ is reduced to DMFc indicates that DMFc engages in cross-phase electron transfer to $Fe(CN)_6^{3-}$ anions in the aqueous phase. The appearance of a cathodic plateau instead of a current peak indicates that a steady-state concentration profile is generated within the NB layer. With a sufficiently high concentration of $Fe(CN)_6^{3-}$ in the aqueous phase, the concentration of DMFc at the NB/H_2O interface becomes negligibly small and the corresponding cathodic plateau current, i_D, is limited by the diffusion of DMFc and $DMFc^+$ across the NB layer. (In the absence of sufficient supporting electrolyte in the NB phase, migration of the $DMFc^+$ could also become important. We have neglected this possible complication in this report.) Under these conditions, the magnitude of the plateau current can be described by eq 1,

$$i_D = nFAC_{NB}D/\delta \qquad (1)$$

where $n = 1$, F is Faraday's constant, A is the electrode area, C_{NB} is the concentration of DMFc dissolved in the NB layer, D is the diffusion coefficient of DMFc in NB, and δ is the thickness of the layer. The observed cathodic plateau currents, i_{obs}, for a series of $Fe(CN)_6^{3-}$ concentrations are shown in Figure 2E. The currents become independent of the concentrations of

TABLE 1: Bimolecular Rate Constants for Cross-Phase Electron Transfer between Pairs of Redox Reactants in Adjoining NB/H_2O Phases

entry no.	reactant in H_2O phase[a]	$E^f_{H_2O}$,[b] mV	reactant in NB phase c	E^f_{NB},[d] mV	ΔE,[e] mV	k_{et},[f] cm s^{-1} M^{-1}	k'_{et},[g] cm s^{-1} M^{-1}
1	$Fe(CN)_6^{3-}$	185	0.55 mM DMFc [h]	−240	425	0.9	
2	$Fe(CN)_6^{3-}$ [i]	175	0.49 mM DMFc	−90	265	0.8	
3	$Fe(CN)_6^{3-}$	185	0.47 mM DMFc	−145	330	0.9	
4	$Fe(CN)_6^{3-}$ [j]	220	0.40 mM DMFc	−175	395	1.1	
5	$Ru(CN)_6^{4-}$	750	0.37 mM $ZnTPP^+$	690	-60	0.8	0.02
6	$Mo(CN)_8^{4-}$	551	0.22 mM $ZnTPP^+$	690	139	1.7	0.5
7	$Fe(CN)_6^{4-}$	185	0.22 mM $ZnTPP^+$	690	505	1.8	
8	$Fe(CN)_6^{4-}$	560	0.39 mM $CoTPP^{2+}$ [l]	862	302	0.2	
9	$IrCl_6^{2-}$ [k]	715	0.18 mM Fc [l]	185	530	1.4	
10	Fe^{2+} [m]	450	0.32 mM $ZnTPP^+$	730	280	0.05	0.06

[a] Supporting electrolyte: 0.1 M $NaClO_4$ + 0.1 M NaCl except where indicated. [b] Formal potential of the reactant redox couple in the H_2O phase vs a saturated calomel electrode as measured by cyclic voltammetry at the bare EPG electrode in the H_2O phase. [c] Supporting electrolyte: 0.25 M THAP except where indicated. [d] Apparent formal potential of the reactant redox couple in the NB phase vs a saturated calomel electrode in the H_2O phase containing the indicated supporting electrolyte as measured by cyclic voltammetry. [e] The driving force of the reaction: $(E^f_{H_2O} - E^f_{NB})$ with the oxidant in the H_2O phase; $(E^f_{NB} - E^f_{H_2O})$ with the oxidant in the NB phase. [f] Evaluated from the slope of plots such as the one in Figure 2F using eqs 2 and 3. [g] Evaluated from data in ref 3c for the H_2O/benzene interface extrapolated to the same driving force. [h] No supporting electrolyte was added to the NB phase. The difference between E^f_{NB} for entries 1 and 2 indicates that $NaClO_4$ partitions into the NB phase to produce a concentration of ca. 0.3 mM. [i] Supporting electrolyte: 0.01 M $NaClO_4$ + 0.1 M NaCl. [j] Supporting electrolyte: 1 M $NaClO_4$ + 0.1 M NaCl. [k] Supporting electrolyte: 2 M $HClO_4$. [l] No supporting electrolyte was added to the NB phase. pH titration showed that the NB phase contained ca. 2 mM $HClO_4$. [m] Supporting electrolyte: 0.01 M $NaClO_4$ + 0.1 M NaCl + 0.5 M H_2SO_4.

$Fe(CN)_6^{3-}$ above about 6 mM. The limiting value of the plateau current at this point, 33 μA, compares favorably with the value of 31 μA calculated from eq 1 using $A = 0.32$ cm^2, $C_{NB} = 0.55$ mM, $D = 6 \times 10^{-6}$ cm^2 s^{-1},[4] and $\delta = 3.2 \times 10^{-3}$ cm (calculated from the volume of NB used to prepare the thin layer.[4])

The reasonable agreement between the calculated and observed values of the limiting plateau current is evidence that the current is controlled by the diffusion of DMFc in the NB phase. The plateau currents remained essentially the same when the concentrations of the supporting electrolyte were varied between 0.01 and 1 M $NaClO_4$ in the aqueous phase and between 0 and 0.25 M THAP in the NB phase. This behavior was consistent with the fact that no ion transfer across NB/H_2O takes place when the currents are measured at steady state. In the absence of added electrolyte in the NB phase, $NaClO_4$ is presumed to partition from the aqueous phase into the NB layer (perhaps driven by the oxidation of DMFc to $DMFc^+$ at the initial electrode potential). The quantity of $NaClO_4$ present in the NB phase was sufficient to prevent distortion of the responses by ohmic drops in the thin layer of NB.

The forward and reverse traces in Figure 2D would be expected to be superimposable if true steady-state currents were involved. The hysterysis in the solid curve in Figure 2D resulted from the finite scan rate (5 mV s^{-1}) at which the curve was recorded. When the currents were recorded point-by-point, i.e., at a scan rate of 0 mV s^{-1}, they were independent of the direction of the changes in potential (plotted points in Figure 2D).

With concentrations of $Fe(CN)_6^{3-}$ less than ~6 mM, smaller plateau currents are obtained (Figure 2E) with magnitudes that are likely to be influenced by the rate of electron transfer from DMFc molecules in the NB phase to $Fe(CN)_6^{3-}$ anions in the aqueous phase. The diffusion of $Fe(CN)_6^{3-}$ anions in the aqueous phase was neglected in the present experiments because, especially at higher concentrations, the magnitudes of the plateau currents were smaller than the peak currents for the diffusion-limited reduction of $Fe(CN)_6^{3-}$ at the uncoated electrode.

It is convenient to use a characteristic current to describe the rate of cross-phase electron transfer at the NB/H_2O interface[3a,7]

$$i_{et} = nFAk_{et}C_{NB}C_{H_2O} \qquad (2)$$

where k_{et} is a bimolecular rate constant (with units of cm s^{-1} M^{-1}) governing electron transfer between the two reactants present at concentrations C_{NB} and C_{H_2O} in the NB and aqueous phases, respectively, and the reaction rate is assumed to be first order in both reactants. The observed plateau current, i_{obs}, should then be described by eq 3,[7] from which i_{et} can be obtained

$$\frac{1}{i_{obs}} = \frac{1}{i_D} + \frac{1}{i_{et}} \qquad (3)$$

because i_D can be calculated from eq 1 or measured as in Figure 2E. According to eqs 1 and 3, a plot of $(i_{obs})^{-1}$ vs $(C_{H_2O})^{-1}$ should be linear with a slope inversely proportional to $k_{et}C_{NB}$ and an intercept equal to $(i_D)^{-1}$. Shown in Figure 2F are two such plots for the DMFc/$Fe(CN)_6^{3-}$ reactant pair. The plots are reasonably linear, and the slopes of the lines correspond to values of k_{et} that are in reasonable agreement, 0.9 and 0.8 cm s^{-1} M^{-1}. The intercept of the lower line in Figure 2F corresponds to a value of 30 μA for i_D, which is in good agreement with the limiting value of the current at the highest concentration of $Fe(CN)_6^{3-}$ in Figure 2E. Thus, the behavior shown in Figure 2F supports the use of eq 3 to analyze data like those in Figure 2E.

Experiments such as those in Figure 2 were repeated with differing concentrations of supporting electrolyte in the aqueous phase and a fixed high concentration of THAP in the NB phase in order to inspect the sensitivity of k_{et} to changes in the driving force of the electron-transfer reaction produced by changes in the Galvani potential difference at the NB/H_2O interface, as elaborated in detail by Wei et al.[3a] The experimental data, available in the Supporting Information, were used to obtain values of the rate constants that are included in the summary compiled in Table 1.

Electron Transfer from Reductants in the Aqueous Phase to $ZnTPP^+$ in the NB Phase. To compare rate constants evaluated with the thin layer and SECM techniques, some of the reactant couples examined previously by Bard and coworkers[3] were also examined. For this purpose, we reacted zinc tetraphenylporphyrin radical cation ($ZnTPP^+$) generated in the NB phase with $Fe(CN)_6^{4-}$, $Mo(CN)_8^{4-}$, or $Ru(CN)_6^{4-}$ anions in the aqueous phase. A typical set of results is shown in Figure 3, which is entirely analogous to Figure 2 except that anodic

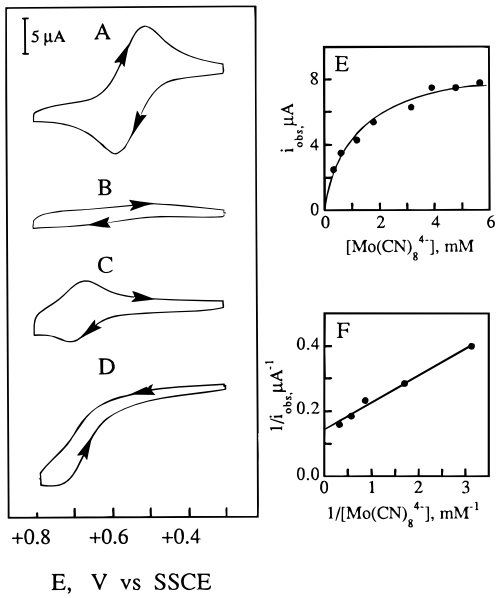

Figure 3. Electron transfer from $Mo(CN)_8^{4-}$ in the aqueous phase to the radical cation of zinc tetraphenylporphyrin ($ZnTPP^+$) in the NB phase. (A) Cyclic voltammogram of 0.5 mM $Mo(CN)_8^{4-}$ at an uncoated EPG electrode: supporting electrolyte, 0.1 M $NaClO_4$ + 0.1 M NaCl; scan rate, 5 mV s^{-1} throughout. (B) Repeat of A after the electrode was covered with a thin layer of NB. (C) Cyclic voltammogram for an electrode covered with 1 μL of NB containing 0.45 mM ZnTPP and 0.25 M THAP. The aqueous solution contained only supporting electrolyte (0.1 M $NaClO_4$ + 0.1 M NaCl). (D) Repeat of C except the NB phase contained 0.1 mM ZnTPP and the aqueous phase contained 3.9 mM $Mo(CN)_8^{4-}$. (E) Anodic plateau currents such as that in D as a function of the concentration of $Mo(CN)_8^{4-}$ in the aqueous phase. (F) Reciprocal plateau currents vs $[Mo(CN)_8^{4-}]^{-1}$.

rather than cathodic plateau currents are obtained. The formal potential of the $ZnTPP^+$/ZnTPP couple in NB obtained from Figure 3C was 0.69 V. This value is somewhat less positive than the value obtained by Tsionsky et al.,[3b] who used benzene as the organic phase. Experimental data like those in Figure 3 were also obtained for the other two reductants and are included in the Supporting Information. The values of k_{et} for all three reactant pairs are given in Table 1.

The concentrations of ZnTPP in the NB layers used in experiments such as those in Figure 3 were purposefully maintained at relatively low values. The higher currents that resulted with higher concentrations of ZnTPP sometimes produced distortions in the steady-state current plateaus. Tsionsky et al. reported similar anomalous behavior in their SECM measurements which they attributed to the formation of precipitates at the benzene/H_2O interface when the concentration of $ZnTPP^+$ in the organic phase was increased.[3b] Under similar conditions we sometimes observed peak-shaped current−potential curves with current magnitudes that exceeded by severalfold the calculated values of i_D for $ZnTPP^+$ in the NB phase. The phenomenon could always be eliminated by diminishing the concentration of $ZnTPP^+$ in the NB, and no current anomalies were observed when the reactant in the NB was neutral instead of cationic (i.e., ferrocene or DMFc). We did not examine the phenomenon in more detail, but we suspect that the formation of precipitates at the NB/H_2O interface may induce convective transport within the NB phase.

Additional Systems. An interesting set of results was obtained with cobalt tetraphenylporphyrin radical cation ($CoTPP^{2+}$) as the electron acceptor in the NB phase. Figure 4 summarizes the experimental data. The noteworthy difference from the behavior of ZnTPP in Figure 3C is the presence of

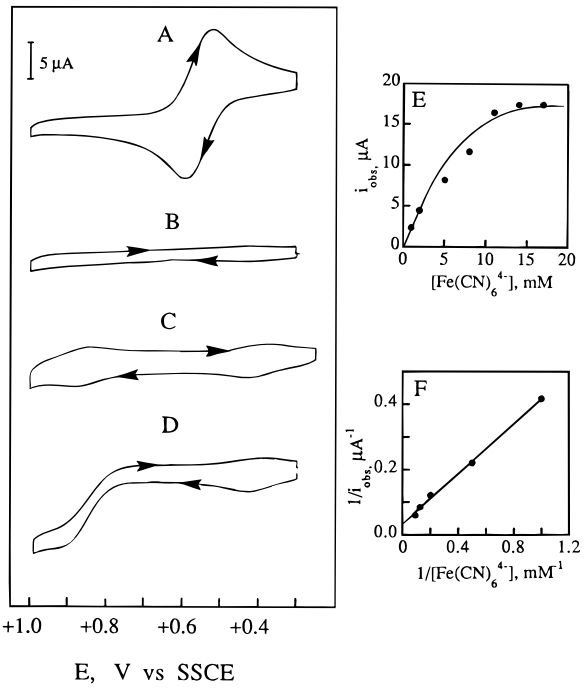

Figure 4. Electron transfer from $Fe(CN)_6^{4-}$ in the aqueous phase to $CoTPP^{2+}$ in the thin layer of NB. (A) Cyclic voltammogram of 0.7 mM $Fe(CN)_6^{4-}$at an uncoated EPG electrode: supporting electrolyte, 2 M $HClO_4$; scan rate, 5 mV s^{-1} throughout. (B) Repeat of A after the electrode was covered with a thin layer of NB. (C) Cyclic voltammogram for an electrode covered with 1 μL of NB containing 0.39 mM CoTPP. The aqueous phase contained only supporting electrolyte (2 M $HClO_4$). (D) Repeat of C with 5.7 mM $Fe(CN)_6^{4-}$ present in the aqueous phase. (E) Anodic plateau currents such as that in D as a function of the concentration of $Fe(CN)_6^{4-}$ in the aqueous phase. The NB phase contained 0.39 mM CoTPP. (F) Reciprocal plateau currents vs $[Fe(CN)_6^{4-}]^{-1}$.

two sets of voltammetric responses from CoTPP in the NB phase (Figure 4C) corresponding to the $CoTPP^+$/CoTPP couple near 0.4 V and the $CoTPP^{2+}$/$CoTPP^+$ couple near 0.9 V. When $Fe(CN)_6^{4-}$ was present in the aqueous phase (Figure 4D), the current in the vicinity of the CoTPP/$CoTPP^+$ couple was not enhanced because $CoTPP^+$ is too weak an oxidant to oxidize $Fe(CN)_6^{4-}$. However, the more strongly oxidizing $CoTPP^{2+}$ cation is capable of accepting an electron from $Fe(CN)_6^{4-}$, and an anodic current plateau is obtained near 0.9 V (Figure 4D). The value of k_{et} calculated from the slope of the line in Figure 4E is given in Table 1.

Analogous experiments with ferrocene in the NB phase and $IrCl_6^{2-}$ in the aqueous phase were also carried out (Supporting Information) to obtain the value of k_{et} for this reactant pair given in Table 1.

Discussion

Method. The simplicity of the method described in this report for evaluating rates of electron transfer between reactants located in different immiscible phases is its most attractive feature. Wei et al. pointed out the variety of potential problems that can be encountered in using conventional electrochemical methods for studying charge-transfer kinetics at the interface between two immiscible liquids.[3a] The alternative SECM method utilized by them has a number of advantages compared with the conventional methods. However, the actual charge-transfer process that is monitored in SECM experiments is more complex because it involves simultaneous electron transfer and ion transfer, while only electron transfer is involved with the

steady-state thin layer procedure described in this report. The method is considerably simpler than previously employed methods because it requires neither a bipotentiostat nor computers for positioning microelectrodes or fitting experimental data to calculated curves. In addition, the steady-state plateau currents used in the evaluation of the rate constants in the thin layer method are not influenced by the kinetics of heterogeneous electron transfer at the electrode surface.

The maximum value of the rate constant, k_{et}, that may be measured with the thin layer method is determined by the relative values of i_D (eq 1) and i_{et} (eq 2). If it is assumed that the slopes of plots based on eq 3 would allow i_{et} to be evaluated as long as $i_{et} < \sim 10 i_D$, the maximum value of k_{et} would be given by $10D/C_{H_2O}\delta$. With a 20 μm layer of nitrobenzene, a diffusion coefficient of the reactant in NB of 6×10^{-6} cm^2 s^{-1}, and a reactant concentration of 10^{-3} M in the aqueous phase, the calculated upper limit on measurable values of k_{et} is 30 cm s^{-1} M^{-1}, which compares very favorably with upper limits available from previously employed procedures. This upper limit could be raised if it proved possible to employ thinner layers of the organic phase.

In their report, Wei et al.[3a] discussed the possibility of measuring interfacial charge-transfer rates by using thin layers of one solvent trapped at the surface of microelectrode tips that were immersed in a second, immiscible solvent, but no experimental examples were presented. The discovery that stable, thin layers of organic solvents are easy to deposit and retain on conventional graphite electrodes was the key to the development of the approach described in this report.

Results. Values of bimolecular rate constants for the cross-phase electron-transfer processes examined in this study are summarized in Table 1. Some of the same reactant pairs were examined previously by Bard and co-workers using benzene instead of nitrobenzene as the organic phase.[3] In most cases they did not evaluate bimolecular rate constants explicitly, but values estimated from their data are also given in Table 1. The dielectric constants of the two solvents, 2.2 and 34 for benzene and NB, respectively, are so different that some of the differences in the values of the rate constants obtained in the two studies might be attributed to this factor. The data in Table 1 for the oxidation of $Ru(CN)_6^{4-}$, $Mo(CN)_8^{4-}$, and $Fe(CN)_6^{4-}$ by $ZnTPP^+$ show a lower sensitivity of the rate constant to the driving force of the reaction than was observed by Tsionsky et al. with the $ZnTPP^+$ generated in benzene.[3b] The origin of this difference is unclear although, as pointed out above, the overall reactions investigated in the two studies are different because of the cross-phase transfer of perchlorate anions that accompanied the electron transfer in the experiments of Tsionsky et al. but not in the present experiments. In addition, interactions of the highly charged anions in the aqueous phase with the cation of the supporting electrolyte can decrease their reactivity in electron-transfer reactions.[8]

When the driving force for the reduction of $Fe(CN)_6^{3-}$ in the aqueous phase by DMFc in the NB phase was varied by changing the concentration of $NaClO_4$ in the aqueous phase, there was very little change in the values of k_{et} (entries 2−4 in Table 1). This behavior could be an indication that the actual electron transfer was not cross-phase but involved a small quantity of DMFc that had partitioned into the aqueous phase. Hanzlik et al. contemplated the same possibility for the ferrocene/$Fe(CN)_6^{3-}$ reactant pair.[9] Experiments such as those in entries 1−4 in Table 1 may provide a useful means for distinguishing between cross-phase and in-phase electron transfer.

Additional measurements will clearly be needed to identify with certainty the reasons for the trends in the rate constants collected in Table 1. The use of thin layers of organic solvents as described in this report may facilitate such measurements.

Acknowledgment. This work was supported by the National Science Foundation. It is a pleasure to draw attention to the fact that the work described in the present paper, as has so much other research on charge transfer at interfaces, benefited significantly from the stimulating ideas and experimental innovations which have emanated from Prof. Allen J. Bard and his research group.

Supporting Information Available: Figures similar to Figure 3 containing the experimental data that were used to complete entries 2−4, 5, 7, 9, and 10 in Table 1 (7 pages). Ordering information is given on any current masthead page.

References and Notes

(1) (a) Girault, H. H.; Schiffrin, D. J. In *Electroanalytical Chemistry*; Bard, A. J., Ed.; Marcel Dekker: New York, 1989; Vol. 15, p 1. (b) Girault, H. H. In *Modern Aspects of Electrochemistry*; Bockris, J. O'M., Conway, B. E., White, R. E., Eds.; Plenum Press: New York, 1993; Vol. 25, p 1.

(2) (a) Bard, A. J.; Denuault, C.; Lee, C.; Mandler, D.; Wipf, D. O. *Acc. Chem. Res.* **1990**, *23*, 357. (b) Bard, A. J.; Fan, F.-R. F.; Mirkin, M. F. In *Electroanalytical Chemistry*; Bard, A. J., Ed.; Marcel Dekker: New York, 1994; Vol. 18. (c) Bard, A. J.; Fan, F.-R. F.; Mirkin, M. V. *Physical Electrochemistry: Principles, Methods and Applications*; Rubinstein, I., Ed.; Marcel Dekker: New York, 1995.

(3) (a) Wei, C.; Bard, A. J.; Mirkin, M. V. *J. Phys. Chem.* **1995**, *99*, 16033. (b) Tsionsky, M.; Bard, A. J.; Mirkin, M. V. *J. Phys. Chem.* **1996**, *100*, 17881. (c) Tsionsky, M.; Bard, A. J.; Mirkin, M. V. *J. Am. Chem. Soc.* **1997**, *119*, 10785. (d) Delville, M.-H.; Tsionsky, M.; Bard, A. J. *Langmuir* **1998**, *14*, 2774.

(4) Shi, C.; Anson, F. C. *Anal. Chem.* **1998**, *70*, 3114.

(5) (a) Geblewicz, G.; Schiffrin, D. J. *J. Electroanal. Chem.* **1988**, *244*, 27. (b) Cunnane, V. J.; Schiffrin, D. J.; Beltran, C.; Geblewicz, G.; Solomon, T. *J. Electroanal. Chem.* **1988**, *247*, 203. (c) Cheng, Y.; Schiffrin, D. J. *J. Electroanal. Chem.* **1991**, *319*, 153.

(6) Connelly, N. G.; Geiger, W. E. *Chem. Rev.* **1996**, *96*, 877.

(7) Andrieux, C. P.; Savéant, J.-M. In *Molecular Design of Surfaces*; Murray, R. W., Ed.; John Wiley & Sons: New York, 1992.

(8) Bindra, P.; Gerischer, H.; Peter, L. M. *J. Electroanal. Chem.* **1974**, *57*, 435.

(9) Hanzlik, J.; Samec, Z.; Hovorka, J. *J. Electroanal. Chem.* **1987**, *216*, 303.